The hydrolysis products of *cis*-diamminedichloroplatinum(II)
4. Metal ion assisted aquation of *cis*-$PtCl_2(NH_3)_2$ and the structure of [*cis*-$PtCl_2(NH_3)_2\cdot(HgCl_2)_3]_n$

Sian E. Miller, Huo Wen, Donald A. House* and Ward T. Robinson*
Department of Chemistry, University of Canterbury, Christchurch (New Zealand)

(Received October 11, 1990; revised January 14, 1991)

Abstract

Chloride release from *cis*-$PtCl_2(NH_3)_2$ dissolved in 0.1 M $HClO_4$ is accelerated by the addition of either $HgCl_2$ or Pb^{2+}. Kinetic parameters associated with the second-order reactions are: k_{HgCl_2} (25 °C)$=1.07\times10^{-2}$ M^{-1} s^{-1}, $\Delta H^{\ddagger}=67.9$ kJ mol^{-1} and $\Delta S^{\ddagger}=-55$ J K^{-1} mol^{-1}, independent of [H^+] (0.1–1.0 M) or ionic strength (0.1–1.0 M); k_{Pb} (25 °C)$=3.72\times10^{-4}$ M^{-1} s^{-1}, $\Delta H^{\ddagger}=85.5$ kJ mol^{-1} and $\Delta S^{\ddagger}=-24$ J K^{-1} mol^{-1} ($I=1.0$ M). For Pb^{2+}, the final product is *cis*-$PtCl(NH_3)_2(OH_2)^+$, but for $HgCl_2$ the final products are *cis*-$Pt(NH_3)_2(OH_2)_2^{2+}$ and $HgCl_4^{2-}$ with this mixture forming crystals of *cis*-$\{PtCl_2(NH_3)_2\cdot(HgCl_2)_3\}_n$ at long reaction times. In this polymer (monoclinic, *C*2/*c*, $a=18.532(5)$, $b=6.506(2)$, $c=12.492(4)$ Å, $\beta=98.76(3)$°, $V=1485.5(8)$ Å^3, $Z=4$, $D_{calc}=4.98$ g/cc) each chloro ligand of the *cis*-$PtCl_2(NH_3)_2$ unit is linked by Pt–Cl–Hg bridges to $HgCl_2$ molecules to form a chain (Cl...Hg=3.004(4) Å). An additional $HgCl_2$ molecule is linked (Cl...Hg=2.979(4) Å) to each of the bridging chloro ligands to give $\{PtCl_2(NH_3)_2\cdot(HgCl_2)_3\}_n$ as the repeat unit.

Introduction

cis-Diamminedichloroplatinum(II) is widely used in antitumor cancer therapy [1]. We are currently studying the hydrolysis kinetics of this compound and the anation kinetics of the products, under a variety of pH and ionic strength conditions [2–4]. In acid conditions, the rate of loss of the first chloro ligand (k_1, eqn. (1)) has a half-life of about 3.0 h at 25 °C, independent of ionic strength (0.01–1.0 M) and hydrogen ion concentration (0.01–1.0 M) [2].

$$cis\text{-}PtCl_2(NH_3)_2 \underset{k_{-1}}{\overset{k_1}{\rightleftharpoons}} cis\text{-}PtCl(NH_3)_2(OH_2)^+ + Cl^- \quad (1)$$

The second chloro ligand is not lost under these conditions, due to the unfavourable equilibrium constant ($K_2=k_2(k_{-2})^{-1}$) associated with eqn. (2), although a value for k_2 can be obtained from a knowledge of k_{-2} and K_2 [3].

$$cis\text{-}PtCl(NH_3)_2(OH_2)^+ \underset{k_{-2}}{\overset{k_2}{\rightleftharpoons}} cis\text{-}Pt(NH_3)_2(OH_2)_2^{2+} + Cl^- \quad (2)$$

A chemical procedure to accelerate chloride release from relatively inert transition metal chloro complexes is to add a metal ion (M^{n+}) which forms a strong M–Cl bond, e.g. Hg^{2+}, Tl^{3+} or Pb^{2+}, or which precipitates an insoluble MCl_x salt, e.g. Ag^+ or Hg_2^{2+}. Most kinetic studies in this area [5] involve either Hg^{2+} or Tl^{3+} as the metal ion assisting the halide release [6] because the formation of a precipitate limits the methods available to monitor the reaction and heterogeneous systems are often subject to complicating surface effects. Nevertheless, the addition of stoichiometric quantities of Ag^+ to *cis*-$PtCl_2(NH_3)_2$, followed by filtration of the AgCl, is the standard synthetic route to produce *cis*-$Pt(NH_3)_2(OH_2)_2^{2+}$ in solution [7a].

Our attempts to measure the Hg^{2+} assisted hydrolysis of *cis*-$PtCl_2(NH_3)_2$ using spectrophotometric techniques were thwarted by the high UV absorbance (345–230 nm) of Hg^{2+} solutions in HNO_3 or $HClO_4$ but we have found that $HgCl_2$ or PbO, dissolved in $HClO_4$, are sufficiently transparent in this region to enable kinetic measurements to be made.

Experimental

cis-Diamminedichloroplatinum(II) was purchased from Strem Chemical Co. and used as supplied. All

---

*Authors to whom correspondence should be addressed.

0020-1693/91/$3.50

other chemicals were AR quality or the best Reagent Grade available.

Kinetics

Solutions of $HgCl_2$ (22.1–36.8 mM) in various $HClO_4$:$NaClO_4$ media were prepared from weighed amounts of the solid and allowed to reach thermal equilibrium in a temperature controlled water bath. A small sample (5–8 mg) of *cis*-$PtCl_2(NH_3)_2$ was dissolved in a few drops of dimethylformamide (DMF) in a 1.00 cm spectrophotometer cell and this solution was allowed to reach thermal equilibrium in the temperature controlled (± 0.1 °C) cell compartment of a Varian DMS100 recording spectrophotometer. The appropriate $HgCl_2$:$HClO_4$:$NaClO_4$ solution (2.5–3 ml) was then added and, after mixing, the absorbance versus time data were collected at 300 nm (plus 285 and 310 nm if time allowed) at appropriate time intervals. Reactions were monitored for 6–8 half-lives to give a constant absorbance and, as the $[HgCl_2]_i$ was always $\geq 10 \times [Pt(II)]_i$, pseudo-first-order rate constants (k_{obs}, s^{-1}) (Table 1) could be calculated. Second-order rate constants k_{HgCl_2} ($M^{-1}\,s^{-1}$) (Table 1) were obtained from the expression $k_{HgCl_2} = k_{obs}[HgCl_2]_i^{-1}$.

Solutions of Pb^{2+} in $HClO_4$ were prepared by dissolving the appropriate weight of PbO in 1.0 M $HClO_4$. Small samples (~5 mg) of *cis*-$PtCl_2(NH_3)_2$ were dissolved in the thermally equilibrated Pb^{2+} solution in a 1.00 cm spectrophotometer cell and absorbance versus time data were collected at 300 and 260 nm while the spectrophotometer was operating in the repeat scan (350–250 nm) mode.

The pseudo-first-order rate constants so obtained (k'_{obs}, s^{-1}) (Table 2) were plotted against the $[Pb^{2+}]$ (Fig. 1) and values for k_1 (s^{-1}) (eqn. (1)) and k_{Pb} ($M^{-1}\,s^{-1}$) were calculated from the least-squares intercept and slope, respectively (Table 3).

Formation and structure of [cis-$PtCl_2(NH_3)_2 \cdot 3HgCl_2]_n$

To a solution of 0.03 M $HgCl_2$ in 0.1 M $HClO_4$ (20 ml) was added 20 mg of *cis*-$PtCl_2(NH_3)_2$. This mixture was heated at 60 °C for about 2 h and then allowed to cool slowly to room temperature in the dark. Pale yellow needles, suitable for single crystal X-ray analysis, deposited over the next 48 h.

TABLE 1. Spectrophotometrically determined rate constants for the reaction of *cis*-$PtCl_2(NH_3)_2$ in 0.10 M $HClO_4$ containing $HgCl_2$ ($I = 0.1$ M)[a]

$[HgCl_2]_i$ (mM)	T (°C [K])	$10^4 \times k_{obs}$ (s^{-1})	$10^2 \times k_{HgCl_2}$[b] ($M^{-1}\,s^{-1}$)	$10^2 \times k_{HgCl_2}$ (calc.) ($M^{-1}\,s^{-1}$)	
22.1	20.0 [293.2]	1.47(2)	0.665(1)	0.675[c]	0.662[d]
29.5		2.00(3)	0.678(1)		
22.1	25.0 [298.2]	2.05(2)	0.928(1)	0.978	1.07
25.8		2.42(1)	0.938(1)		
29.5		2.98(8)	1.01(1)		
22.1	30.0 [303.3]	4.15(13)	1.88(6)	1.77	1.71
25.8		4.83(2)	1.87(1)		
29.5		5.25(10)	1.78(3)		
33.2		6.00(9)	1.81(3)		
36.8		6.41(4)	1.74(1)		
22.1	35.0 [308.2]	6.09(8)	2.76(4)	2.89	2.70
25.8		7.51(26)	2.91(10)		
29.5		8.33(9)	2.82(3)		
		7.04(4)[e]	2.39(1)		
		8.33(29)[f]	2.82(10)		
		9.67(25)[g]	3.28(9)		
33.2		9.51(5)	2.87(2)		
36.8		10.7(12)	2.91(3)		
22.1	40.0 [313.2]	8.73(1)	3.95(1)	3.87	4.18
25.8		10.1(1)	3.92(1)		
29.5		11.5(10)	3.89(3)		
33.2		12.7(19)	3.84(6)		
36.8		14.3(17)	3.89(5)		

[a] Numbers in parentheses are the uncertainty (standard deviation) in the last digit(s) from >20 data points for each kinetic run. [b] Calculated from the expression $k_{HgCl_2} = k_{obs}[HgCl_2]^{-1}$. [c] Calculated from a linear least-squares analysis of plots of $[HgCl_2]_i$ vs. k_{obs}. [d] Calculated from the activation parameters obtained for k_{HgCl_2}, viz. $\Delta H^{\neq} = 67.9 \pm 2$ kJ mol^{-1} and $\Delta S^{\neq} = -55.0 \pm 4$ J K^{-1} mol^{-1}. [e] $[HClO_4] = 0.01$ M; $[NaClO_4] = 0.99$ M; $I = 1.0$ M. [f] $[HClO_4] = 0.1$ M; $[NaClO_4] = 0.9$ M; $I = 1.0$ M. [g] $[HClO_4] = 1.0$ M; $I = 1.0$ M.

TABLE 2. Observed rate constants ($10^4 \times k'_{obs}$ s^{-1}) for the Pb^{2+} assisted aquation of *cis*-$PtCl_2(NH_3)_2$ ($I = 1.0$ M, $HClO_4$)

$[Pb^{2+}]$ (M)	35.2 °C [308.4 K]	40.2 °C [313.4 K]	45.0 °C [318.2 K]	50.0 °C [323.2 K]
0.02	2.01±0.33 2.01±0.24	3.42±0.33 3.53±0.52	5.62±0.50 5.81±0.69	9.60±0.80 9.29±0.42
0.03	2.12±0.36 2.14±0.45	4.21±0.75 3.96±0.64	6.78±1.2 6.82±1.5	10.4±0.6 10.3±0.6
0.04	2.24±0.29 2.48±0.32	4.32±0.60 4.16±0.45	7.51±0.75 7.07±0.82	11.6±0.8 11.3±0.7
0.06	2.73±0.42 2.68±0.58	4.76±0.20 4.50±0.62	7.79±0.49 7.35±0.54	12.1±0.6 12.0±0.8
0.10	3.04±0.30 3.02±0.88	5.38±0.56 5.49±0.43	9.69±0.94 9.54±1.2	14.1±0.6
0.12	3.24±0.39	5.79±0.49	10.5±0.5 9.46±0.5	15.0±0.2
0.20	4.11±0.48		12.9±0.6	

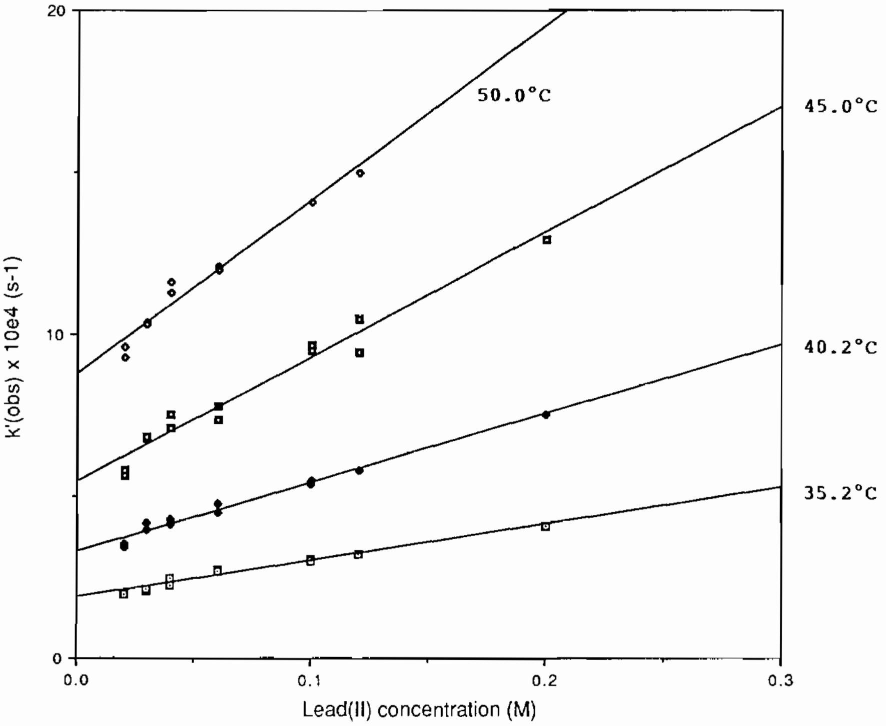

Fig. 1. Plot of $10^4 \times k'_{obs}$ vs. $[Pb^{2+}]$ at various temperatures ($I = 1.0$ M).

Intensity data for a small elongated rod-like crystal (0.10×0.12×0.48 mm) were collected with a Nicolet R3m four-circle diffractometer at −125 °C. Graphite monochromated Mo Kα radiation (0.71060 Å) was used, with fixed ω scans. Cell parameters were determined by least-squares refinement of 25 accurately centered reflections. During the data collection, the intensities of three standard reflections were monitored at regular intervals and these indicated no significant crystal decomposition. The collected intensities were corrected for Lorentz, polarisation and absorption effects (both automatically and from crystal indexing) (Table 4).

The structure was solved by conventional Patterson and Fourier methods and refined by blocked cascade least-squares procedures. The Pt and Hg atoms were

TABLE 3. Rate constants calculated for the Pb^{2+} assisted aquation of *cis*-$PtCl_2(NH_3)_2$ ($I = 1.0$ M)

T (°C)	[K]	$10^3 \times k_{Pb}$ [a] (M^{-1} s^{-1})	$10^3 \times k_{Pb}$(calc) [b] (M^{-1} s^{-1})	$10^4 \times k_1$ [c] (s^{-1})	$10^4 \times k_1$ [d] (s^{-1})
25.0	[298.2]		0.372		
35.2	[308.4]	1.15	1.20	1.88	1.74
40.2	[313.4]	2.12	2.08	3.30	3.33
45.0	[318.2]	3.84	3.46	5.44	5.47
50.0	[323.2]	5.36	5.79	8.78	8.81

[a] Least-squares slope of the k'_{obs} vs. $[Pb^{2+}]$ plots. [b] Calculated from the activation parameters: $\Delta H^{\neq} = 85.5 \pm 7$ kJ mol^{-1}, $\Delta S^{\neq} = -24 \pm 14$ J K^{-1} mol^{-1}. [c] Least-squares intercept of the k'_{obs} vs. $[Pb^{2+}]$ plots. [d] Independently determined [2] for the thermal aquation of *cis*-$PtCl_2(NH_3)_2$ in 1.0 M $HClO_4$.

TABLE 4. Crystal data

Complex	$PtCl_2(NH_3)_2 \cdot (HgCl_2)_3$
Molecular formula	$H_6N_2Cl_8PtHg_3$
Formula weight	1114.53
Space group	monoclinic, $C2/c$
a (Å)	18.532(5)
b (Å)	6.506(2)
c (Å)	12.492(4)
β (°)	98.76(3)
V (Å^3)	1485.5(8)
Z	4
D_{calc} (g/cc)	4.98
Temperature (°C)	−125
F(000)	1859.27
Absorption correction (cm^{-1})	418.21
Transmission factors	0.331, 0.192
Scan mode	ω
Octants	$0,0,-l$; h,k,l
$2\theta_{max}$ (°)	60
Reflections measured	2179
Reflections used	1653
Parameters refined	61
Weighting ($g \times 10^3$)	5.55
R	0.0591
R_w	0.0630

TABLE 5. Non-hydrogen atom coordinates ($\times 10^4$) for *cis*-$\{PtCl_2(NH_3)_2 \cdot (HgCl_2)_3\}_n$

Atom	x	y	z
Hg(1)	0	0	0
Pt(1)	0	2398(2)	2500
Hg(2)	1996(1)	149(1)	−792(1)
Cl(1)	−639(2)	−2911(7)	345(3)
Cl(2)	1503(2)	−2672(7)	−58(4)
Cl(3)	2548(3)	2852(8)	−1537(4)
N(1)	784(9)	4629(26)	2307(14)
Cl(4)	851(2)	−78(7)	2252(4)

distinguished on the basis of chemical reasoning, and all atoms heavier than N were refined with anisotropic thermal parameters (see 'Supplementary material'). In the last cycles of refinement, the appropriate N–H hydrogen atoms were included in their calculated positions. All calculations were performed on a DG30 computer using the SHELXTL [7b] suite of programs and Table 5 lists the non-hydrogen atom coordinates.

Results and discussion

$HgCl_2$ assisted aquation

The spectrophotometric changes that take place on mixing $HClO_4$ solutions of $HgCl_2$ and *cis*-$PtCl_2(NH_3)_2$ are shown in Fig. 2*. Satisfactory isosbestic points were maintained at 275 and 335 nm, indicating a monophasic reaction, and the final absorption spectrum corresponds to that expected for *cis*-$Pt(NH_3)_2(OH_2)_2^{2+}$ dissolved in $HgCl_2$:$HClO_4$ solution. Thus we believe the reaction under investigation corresponds to eqns. (3) and (4) with both chloro ligands on the Pt(II) being displaced simultaneously.

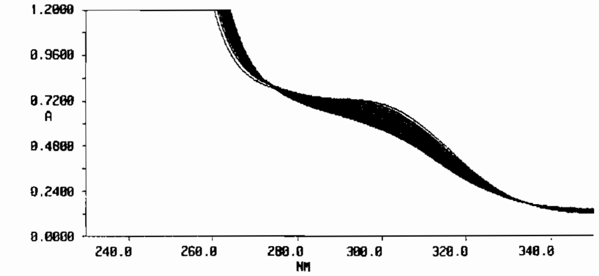

Fig. 2. Spectrophotometric changes associated with the reaction between *cis*-$PtCl_2(NH_3)_2$ ($\sim 2 \times 10^{-3}$ M) and $HgCl_2$ (0.022 M) dissolved in 0.1 M $HClO_4$ at room temperature. The decrease in absorbance at 300 nm corresponds to a repeat scan every 600 s.

---

*Although for most of the data, the Pt(II) complex was dissolved in DMF prior to the addition of the $HClO_4$:$HgCl_2$ solution, experiments without DMF gave entirely similar results.

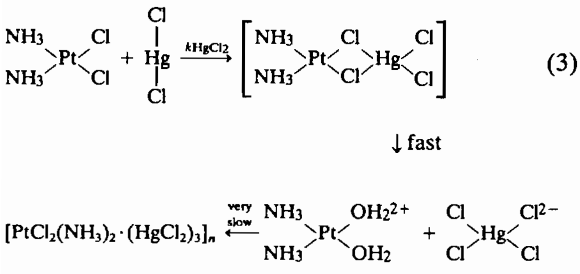

(3)

(4)

The kinetic analysis also supports this conclusion as excellent linear plots of k_{obs} versus $[HgCl_2]_i$ were obtained over a 20 °C temperature range with intercepts at the origin (Fig. 3). Unfortunately, only a limited range of $[HgCl_2]_i$ could be used, as the lower end (0.02 M) was constrained by the $[Pt(II)]_i$ required, and $[HgCl_2]_i$ above 0.04 M resulted in rapid precipitate formation.

The reaction rate is also independent of $[H^+]$ (0.01–1.0 M) and ionic strength (0.01–1.0 M) (Table 1) and activation parameters of $\Delta H^{\neq} = 67.9$ kJ mol^{-1} and $\Delta S^{\neq} = -55.0$ J K^{-1} mol^{-1} were calculated from the variation of k_{HgCl_2} with temperature.

Although $HgCl_2$ is regarded as a rather poor chloride abstractor [5, 8], addition of this reagent to dissolved *cis*-$PtCl_2(NH_3)_2$ certainly facilitates chloride release. Thus, addition of 22.1 mM $HgCl_2$ to 2 mM *cis*-$PtCl_2(NH_3)_2$ reduces the half-life for acid hydrolysis from 3 to 1 h at 25 °C, but significantly different products are formed.

Very few Hg^{2+} assisted halide release reactions have been reported for Pt(II) [5], although (5) and (6) (X = Cl, Br) have been studied spectrophotometrically.

$$Pt(X)(gly)(NH_3) + Hg^{2+} \xrightarrow{k_f} Pt(gly)(NH_3)(XHg)^{2+} \qquad (5)$$

$$Pt(gly)(NH_3)(XHg)^{2+} \xrightarrow{k_d} Pt(gly)(NH_3)(H_2O)^{+} + HgX^{+} \qquad (6)$$

A well defined adduct has been characterised and its rate of formation (k_f) and decomposition (k_d) measured [9]. Although probably fortuitous, the rate of adduct formation ($k_f = 2\times10^{-2}$ M^{-1} s^{-1} at 25 °C) for $PtCl(NH_3)(gly)$ is of similar magnitude to the $HgCl_2$ assisted chloride release rate from *cis*-$PtCl_2(NH_3)_2$ ($k_{HgCl_2} = 1\times10^{-2}$ M^{-1} s^{-1} at 25 °C).

The concept of simultaneous release of both chloro ligands via a cyclic binuclear intermediate of the type shown in eqn. (3) is not new, and similar adducts have been proposed for the Hg^{2+} assisted chloride release from some *cis*-$Co(L_4)Cl_2^+$ complexes [10–12]. Indeed the structure of the binuclear complex *cis*-$[Rh(en)_2Cl_2]Cl\cdot HgCl_2$ clearly shows the formation

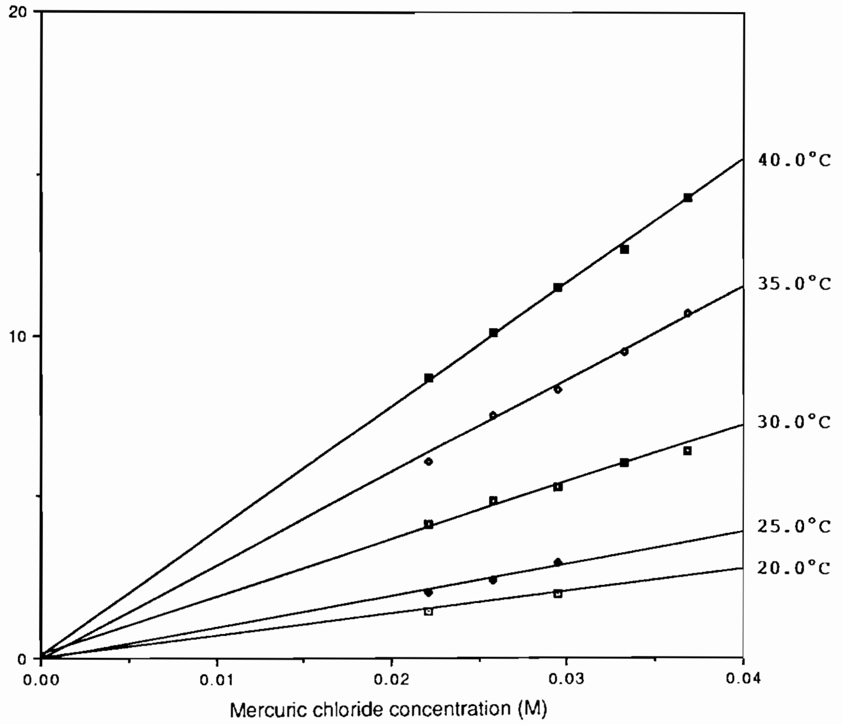

Fig. 3. Plot of $10\times k_{obs}$ (s^{-1}) vs. $[HgCl_2]$ at various temperatures ($I = 1.0$ M).

of a μ-dichloro bridged system [13]. Finally, there are analogous structures reported for square planar, four coordinate, central metal systems which exhibit the metal-μ-dichloromercury(II) bridge system [14, 15]. Note, however, that the end product from the reaction between *cis*-$PtCl_2(NH_3)_2$ and $HgCl_2$, viz. $[PtCl_2(NH_3)_2\cdot(HgCl_2)_3]_n$, contains only platinum-μ-monochloromercury(II) bridges.

Structure of $[PtCl_2(NH_3)_2\cdot(HgCl_2)_3]_n$

Crystals of this product deposit if the contents of the spectrophotometric cell (in the absence of DMF) are allowed to cool overnight. The single crystal X-ray structural analysis shows these to have a polymeric structure (Fig. 4), similar to those reported for $[Et_4N]_2Hg_2PtCl_8$ and $[Et_4N]_2Hg_3PtCl_{10}$ [15]. In $[PtCl_2(NH_3)_2\cdot(HgCl_2)_3]_n$, the *cis*-$PtCl_2(NH_3)_2$ units are linked into chains by bridging of the chloro ligands through an $HgCl_2$ molecule lying on a special position (Cl(4)–Hg(1) = 3.004(4) Å). The chloro ligand bound to Pt is also linked (Cl(4)–Hg(2) = 2.979(4) Å) to a second $HgCl_2$ molecule, whose next closest Hg...Cl interaction is at 3.25 Å, from an equivalent $HgCl_2$ molecule in another chain (Fig. 5). Thus the chloro ligands bound to the Pt(II) are each weakly linked to two $HgCl_2$ molecules.

Bond lengths and angles within the *cis*-$PtCl_2(NH_3)_2$ molecule are similar to those found in isolated *cis*-$PtCl_2(NH_3)_2$ [16] and its DMF adduct [17] (Table 6). The short Hg–Cl distances and the Cl–Hg–Cl angles in both the chain (Hg(1)) and terminal (Hg(2)) $HgCl_2$ molecules are similar to those found in isolated $HgCl_2$ or some of its weaker adducts (Table 7).

The bridging Hg–Cl distances, e.g. Pt–Cl(4)...Hg(1) (3.004(4)) in the chain, or Pt–Cl(4)...Hg(2) (2.979(4)) for the terminal Hg atoms, are well within the sum of the Hg...Cl van der Waals radii (3.25 Å). Other bond lengths and bond angles are listed in Tables 8 and 9.

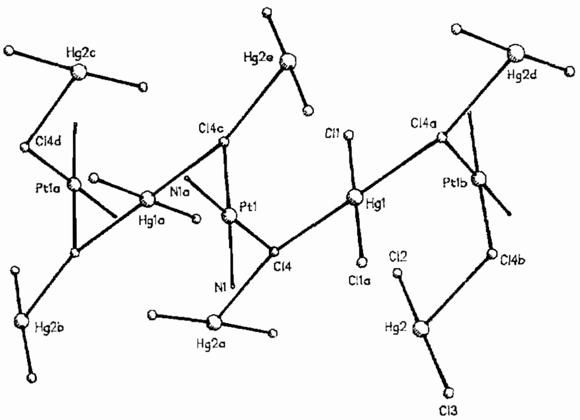

Fig. 4. A view of the $\{PtCl_2(NH_3)_2\cdot(HgCl_2)_3\}_n$ chain showing the atom numbering system adopted.

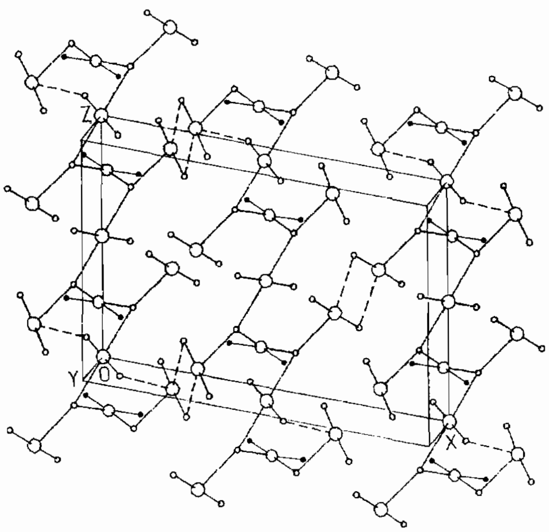

Fig. 5. A packing diagram of $\{PtCl_2(NH_3)_2\cdot(HgCl_2)_3\}_n$.

Pb^{2+} assisted chloride release

Solutions of PbO dissolved in $HClO_4$ are not completely transparent in the 250–350 nm region and as the $[Pb^{2+}]$ increases an increasingly dominant absorbance develops. Consequently, at high $[Pb^{2+}]$, the initial absorption spectra of *cis*-$PtCl_2(NH_3)_2$ dissolved in this media is considerably distorted from that observed in $HClO_4$ alone [3]. Nevertheless, at all Pb^{2+} concentrations, the maxima at 300 nm is maintained and, as the reaction proceeds, this peak decreases in intensity. At low $[Pb^{2+}]$, the *cis*-$PtCl_2(NH_3)_2$ minimum at at ~250 nm is also observed and absorbance in this region increases with increasing time. However, as the Pb^{2+} concentration increases, this initial minimum becomes less well defined and at 0.1 M Pb^{2+} is no longer discernable.

The absorbance of the final product *cis*-$PtCl(NH_3)_2(OH_2)^+$ is also distorted as the $[Pb^{2+}]$ increases. At low $[Pb^{2+}]$, the 263 nm maximum observed in $HClO_4$ alone, is observed, but with increasing Pb^{2+}, the 240 nm minimum is slowly enveloped in the background continuum. At low Pb^{2+}, the reaction proceeds with an isosbestic point at 280 nm, identical in position to the aquation in the absence of Pb^{2+}, but as the $[Pb^{2+}]$ increases, this point becomes less distinct (0.1 M Pb^{2+}) and becomes completely lost at $[Pb^{2+}] \geqslant 0.12$ M.

As Table 2 shows, the aquation rate is increased in the presence of Pb^{2+} and the Pb^{2+} dependence is described by eqn. (7) in the range 0–0.2 M Pb^{2+}.

$$k'_{obs} = k_1 + k_{Pb}[Pb^{2+}] \qquad (7)$$

Plots of $[Pb^{2+}]$ versus k'_{obs} are linear (Fig. 1) with slopes equal to k_{Pb} ($M^{-1}\ s^{-1}$) and intercepts equal to k_1 (s^{-1}), the aquation rate in the absence of Pb^{2+} [2] (Table 3).

TABLE 6. Bond lengths and bond angles in *cis*-$PtCl_2(NH_3)_2$ and its adducts[a]

Complex	Pt–Cl (Å)	Pt–N (Å)	Cl–Pt–Cl (°)	N–Pt–N (°)	Reference
cis-$PtCl_2(NH_3)_2$	2.33(1)×2	2.01(1)×2	91.9(3)	87(1.5)	16
cis-$PtCl_2(NH_3)_2\cdot$DMF	2.315(7) 2.306(7)	2.00(2) 2.08(2)	92.4(3)	91.0(7)	17
cis-$\{(PtCl_2(NH_3)_2\cdot(HgCl_2)_3\}_n$	2.307(5) 2.308(5)	2.093(17)×2	91.5(2)	92.2(1.0)	this work

[a] See also ref. 18 for the structure of *cis*-$PtCl_2(NH_3)_2\cdot$DMA$\cdot$(18-crown-6)$_{1/2}$.

TABLE 7. Bond lengths and bond angles in $HgCl_2$ and some adducts

Compound	Hg–Cl (Å)	Hg...Cl (Å)	Cl–Hg–Cl (°C)	Reference
$HgCl_2$ (cryst.)	2.284(12) 2.301(14)	3.37	178.9(5)	19
$HgCl_2$ (gas)	2.252(5)×2		180(16)	20
$HgCl_2$ (encapsulated)	2.327(7) 2.304(7)		172.7(2)	21
$[H_4ttf][HgCl_2]_3$	2.309(5)×2	2.989(6)×2 3.235(5)×2	180	22
$[DMSO]_2[HgCl_2]_3$	2.306(6)×2	3.004(5)×2 3.081(6)×2	180	23
$[HgCl_2]$ 'chain'	2.308(5)×2	3.004(4)×2	180	this work
$[HgCl_2]$ 'terminal'	2.301(5) 2.300(5)	2.979(4)	176.6(2)	this work

TABLE 8. Bond lengths (Å) in $\{cis\text{-}PtCl_2(NH_3)_2\cdot(HgCl_2)_3\}_n$

Hg(1)–Cl(1)	2.308(5)	Hg(1)–Cl(4)	3.004(4)
Hg(1)–Cl(1A)	2.308(5)	Hg(1)–Cl(4A)	3.004(4)
Pt(1)–N(1)	2.093(17)	Pt(1)–Cl(4)	2.307(5)
Pt(1)–N(1A)	2.093(17)	Pt(1)–Cl(4C)	2.308(5)
Hg(2)–Cl(2)	2.301(5)	Hg(2)–Cl(3)	2.300(5)
Hg(2)–Cl(4B)	2.979(4)		
Cl(4)–Hg(2A)	2.979(4)		

TABLE 9. Bond angles (°) for $\{cis\text{-}PtCl_2(NH_3)_2\cdot(HgCl_2)_3\}_n$

Cl(1)–Hg(1)–Cl(1A)	180.0(1)
Cl(1)–Hg(1)–Cl(4A)	88.7(1)
Cl(1A)–Hg(1)–Cl(4A)	91.3(1)
N(1)–Pt(1)–N(1A)	92.2(10)
N(1)–Pt(1)–Cl(4C)	178.8(4)
N(1A)–Pt(1)–Cl(4C)	88.2(5)
Cl(2)–Hg(2)–Cl(4B)	92.1(1)
Hg(1)–Cl(4)–Pt(1)	80.9(1)
Pt(1)–Cl(4)–Hg(2A)	108.5(2)
Cl(1)–Hg(1)–Cl(4)	91.3(1)
Cl(4)–Hg(1)–Cl(1A)	88.7(1)
Cl(4)–Hg(1)–Cl(4A)	180.0(1)
N(1)–Pt(1)–Cl(4)	88.2(5)
Cl(4)–Pt(1)–N(1A)	178.8(4)
Cl(4)–Pt(1)–Cl(4C)	91.5(2)
Cl(2)–Hg(2)–Cl(3)	176.6(2)
Cl(3)–Hg(2)–Cl(4B)	89.2(1)
Hg(1)–Cl(4)–Hg(2A)	166.5(2)

The acceleratory influence of Pb^{2+} is not large (a rate increase of about 2.3 is observed in a 0.2 M Pb^{2+}, 0.58 M $HClO_4$ solution, relative to 1.0 M $HClO_4$), suggesting only weak Pt–Cl...Pb interaction. Indeed, the activation energies for the two processes agree within experimental error and the only driving force for the Pb^{2+} assisted reaction is a slight increase in the activation entropy.

This reinforces the previous observations [24–26] that Pb^{2+} is not a particularly effective metal ion for Cl^- abstraction.

Other metal ions

The rate of *cis*-$PtCl_2(NH_3)_2$ aquation in 1.0 M $HClO_4$ solution was not increased by the addition of Cu^{2+}, Zn^{2+}, Ca^{2+} or Mg^{2+} (all at the 0.3 M concentration).

We also explored the possibility of metal ion assisted base hydrolysis using solutions of $ZnCl_2$ dissolved in NaOH but the rate in 1.0 M NaOH [3] was not changed in the presence Zn^{2+} in the range 0.02–0.08 M.

Supplementary material

Tables of structure factors, hydrogen atom coordinates and anisotropic thermal parameters are available from D.A.H. or W.T.R.

Acknowledgements

We thank the New Zealand Universities Grants Committee for funds to purchase instruments used in this research, and Huo Wen thanks the same organisation for the award of a post-graduate fellowship.

References

1 A. W. Prestayko, S. T. Crooke and S. K. Carter (eds.), *Cisplatin: Current Status and New Developments,* Academic Press, New York, 1980.

2 S. E. Miller and D. A. House, *Inorg. Chim. Acta, 161* (1989) 131.

3 S. E. Miller and D. A. House, *Inorg. Chim. Acta, 166* (1989) 189.

4 S. E. Miller and D. A. House, *Inorg. Chim. Acta, 173* (1990) 53.

5 R. Banerjee, *Coord. Chem. Rev., 68* (1985) 145.

6 D. A. House, *Coord. Chem. Rev., 23* (1977) 233.

7 (a) J. Arpalahti and B. Lippert, *Inorg. Chem., 29* (1990) 104; (b) G. M. Sheldrick, *SHELXTL User Manual,* Revision 5, Nicolet XRD Corp., Madison, WI, 1986.

8 J. H. Espenson and J. P. Birk, *Inorg. Chem., 4* (1965) 527.

9 A. B. Venediktov and A. V. Belyaev, *Chem. Abstr., 80* (1974) 115565; *81* (1974) 30115; *83* (1975) 121395.

10 C. Bifano and R. G. Linck, *Inorg. Chem., 7* (1968) 908.

11 J. H. Worrell, *Inorg. Chem., 14* (1975) 1699.

12 J. H. Worrell and C. R. Fortune, *J. Inorg. Nucl. Chem., 33* (1971) 3571.

13 N. V. Podberezskaya, A. V. Belyaev and V. V. Bakakin, *Zh. Strukt. Khim., 22* (1981) 32; *Chem. Abstr., 96* (1982) 134794.

14 R. W. Baker, M. J. Braithwaite and R. S. Nyholm, *J. Chem. Soc., Dalton Trans.,* (1972) 1924.

15 R. M. Barr, M. Goldstein, T. N. D. Hairs, N. McPartlin and A. J. Markwell, *J. Chem. Soc., Chem. Commun.,* (1974) 221.

16 G. H. W. Milburn and M. R. Truter, *J. Chem. Soc. A,* (1966) 1609.

17 G. Raudaschl, B. Lippert, J. D. Hoeschele, H. E. Howard-Lock, C. J. L. Lock and P. Pilon, *Inorg. Chim. Acta, 106* (1985) 141.

18 D. R. Alston, J. F. Stoddart and D. J. Williams, *J. Chem. Soc., Chem. Commun.,* (1985) 532.

19 V. Subramanian and K. Seff, *Acta Crystallogr., Sect. B, 36* (1980) 2132.

20 K. Kashiwabara, A. Konaka and M. Kimura, *Bull. Chem. Soc. Jpn., 46* (1973) 410.

21 S. Akabori, H. Munegumi, Y. Habata, S. Sato, K. Kawazoe, C. Tamura and M. Sato, *Bull. Chem. Soc. Jpn., 58* (1985) 2185.

22 M. D. Glick, W. H. Ilsley and A. R. Siedle, *Inorg. Chem., 20* (1981) 3819.

23 P. Biscarini, L. Fusina, G. Nivellini and G. Pelizzi, *J. Chem. Soc., Dalton Trans.,* (1977) 664; (1981) 1024.

24 R. Dyke and W. C. E. Higginson, *J. Chem. Soc. A,* (1963) 2788.

25 S. P. Tanner and W. C. E. Higginson, *J. Chem. Soc. A,* (1969) 1164.

26 H. M. Comely and W. C. E. Higginson, *J. Chem. Soc., Dalton Trans.,* (1972) 2522.